MOLECULAR PHYSICS, 2000, VOL. 98, NO. 20, 1639–1658

What correlation effects are covered by density functional theory?

YUAN HE, JÜRGEN GRÄFENSTEIN, ELFI KRAKA and DIETER CREMER*

Department of Theoretical Chemistry, Göteborg University, Reutersgatan 2, S-41320 Göteborg, Sweden

(*Received 7 June 2000; accepted 15 June 2000*)

The electron density distribution $\rho(\mathbf{r})$ generated by a DFT calculation was systematically studied by comparison with a series of reference densities obtained by wavefunction theory (WFT) methods that cover typical electron correlation effects. As a sensitive indicator for correlation effects the dipole moment of the CO molecule was used. The analysis reveals that typical LDA and GGA exchange functionals already simulate effects that are actually reminiscent of pair and three-electron correlation effects covered by MP2, MP4, and CCSD(T) in WFT. Correlation functionals contract the density towards the bond and the valence region thus taking negative charge out of the van der Waals region. It is shown that these improvements are relevant for the description of van der Waals interactions. Similar to certain correlated single-determinant WFT methods, BLYP and other GGA functionals underestimate ionic terms needed for a correct description of polar bonds. This is compensated for in hybrid functionals by mixing in HF exchange. The balanced mixing of local and non-local exchange and correlation effects leads to the correct description of polar bonds as in the B3LYP description of the CO molecule. The density obtained with B3LYP is closer to CCSD and CCSD(T) than to MP2 or MP4, which indicates that the B3LYP hybrid functional mimics those pair and three-electron correlation effects, which in WFT are only covered by coupled cluster methods.

1. Introduction

Density functional theory (DFT) [1–3] has become one of the most frequently used tools in quantum chemistry for the description of atoms, molecules, and chemical reaction systems. An impressive number of applications of DFT have proven its usefulness and reliability [4]. In particular, the favourable cost–efficiency ratio of DFT and its wide applicability are the reasons why wavefunction theory (WFT) based methods such as Hartree–Fock (HF) theory, Møller–Plesset (MP) perturbation theory [5, 6] at second order (MP2) including just double (D) excitations, at third order (MP3) or at fourth order (MP4), including single (S), D, triple (T) and quadruple (Q) excitations, were more and more replaced by DFT methods in the last decade.

There is, however, one aspect of DFT, which has hampered its acceptance by quantum chemists for a long time. Contrary to WFT methods, DFT does not offer a systematic way of improving the Hamiltonian and in particular the exchange–correlation (XC) potential such that a correct description of all many-particle interactions in a molecule can be approximated in a stepwise, well defined manner. In WFT, this goal is accomplished by extending the single-particle, single-determinant description of HF systematically by introducing higher and higher dynamic electron correlation effects, e.g. with the help of MPn [5, 6] or coupled cluster (CC) theory [7, 8] while in parallel nondynamic electron correlation is introduced by multi-determinant, multi-reference (MR) descriptions such as MR-CI or MR-CC theory [9]. Also, in WFT there is the possibility of specifying those many-particle correlations introduced by a given WF method. [6] For example, MP2 is known to describe electron pair correlation in a somewhat exaggerated way, MP3 corrections pair correlation effects at MP2 by a coupling between D excitations, and MP4 introduces orbital relaxation effects (via the S excitations), three-electron correlation effects (via T excitations), and disconnected four-electron correlation effects via Q excitations. Higher order correlation effects as they are introduced at fifth order (MP5) and sixth order MP theory (MP6) were described by Cremer and coworkers [10–12]. Although MP theory is problematic in its application because of frequent initial oscillations in the MPn series [13], it provides a platform for analysing electron correlation effects [14, 15] covered by more advanced methods such as CCSD [16] or CCSD(T) [17]. For example, the former method

* Author for correspondence. e-mail: cremer@theoc.gu.se

Table 1. Overview over exchange and correlation functionals used in this work.

Name	Abbrev.	Local	Non-local	Ref.
A. Exchange functionals				
Slater	S	(exact) E_x from the homogeneous electron gas (HEG)	none	[18]
Becke 88	B	as Slater	correction term with one empirical parameter, which by construction (adjustment to exact HF exchange) corrects the asymptotical behaviour of $\varepsilon_X(\mathbf{r})$	[19]
Perdew–Wang 91	PW91	as Slater	correction term based on the exchange hole in a weakly inhomogeneous electron gas and some rigorous relations for E_x	[20]
Modified PW (Barone)	mPW	as Slater	based on PW91, readjusting some parameters to improve the performance in the low-density limit; adjustment is done with a fit to noble-gas dimers	[21]
B. Correlation functionals				
Vosko–Wilk–Nusair	VWN	RPA for the HEG (i.e. doubles)	none	[22]
Vosko–Wilk–Nusair V	VWN5	Quantum Monte Carlo (QMC) for the HEG (i.e. all excitations)	none	[22]
Perdew Local	PL	QMC for the HEG (i.e. all excitations)	none	[23]
Perdew 86	P86	QMC for the HEG (i.e. all excitations)	C hole for the weakly inhomogeneous electron gas	[23, 24]
Perdew–Wang 91	PW91	QMC for the HEG (i.e. all excitations)	C hole for the weakly inhomogeneous electron gas	[20]
Lee–Yang–Parr	LYP	derived by a fit to the He atom (i.e. no separation between local and non-local part)		[25]

contains all infinite order effects in the SD space, which means that for $2 \leqslant n \leqslant \infty$ all MPn energy terms built up by just S and D are automatically covered as well as many (disconnected) higher order contributions [14]. Similarly, CCSD(T) covers (up to MP8) 77% of the terms of the SDT space of the more complete CCSDT method [15]. Hence, the systematic extension of MP and CC theory provides a firm basis for the understanding of the stepwise improvement of these methods.

DFT covers an unspecified amount of dynamic electron correlation effects introduced by the XC functional (see table 1) [18–29]. If the correlation functional was constructed from the homogeneous electron gas (HEG) using quantum Monte Carlo (QMC) methods [22], actually all possible correlation effects should be included. However, the electron density distribution of atoms and molecules is inhomogeneous and contains besides local also non-local correlation. At the DFT level, the latter effects can be accounted for only in an approximate way and, by this, it is no longer clear which correlation effects are covered by a given correlation functional.

In this connection it has to be noted that DFT exchange and correlation functionals are designed such that they together allow for a reasonably correct description of the exchange and Coulomb correlation effects in an electron system, but not to give an accurate account of exchange and correlation effects separately. In particular, correlation functionals were developed in many cases to complement a particular exchange functional. Besides this practical aspect one has to be aware that the exact exchange and correlation energies of DFT and WFT are conceptually different. Whereas the exact HF exchange is calculated from the HF Slater determinant constructed from energy-optimized HF orbitals, the exact KS exchange energy is based on the Slater determinant formed from the Kohn–Sham (KS) orbitals. The KS orbitals in turn are determined in such a way that they reproduce the electron density of the real electron system, which means that the true KS orbitals account for all electron correlation effects in the molecule. In this sense, the KS exchange energy calculated with the help of the KS orbitals is influenced by the electron correlation in the system even though it is calculated from the wavefunction of a non-interacting reference system. As regards the correlation energy, it is defined as the difference between the exact energy of the interacting many-electron system and the energy of a suitable reference system, which in WFT is given by the HF description.

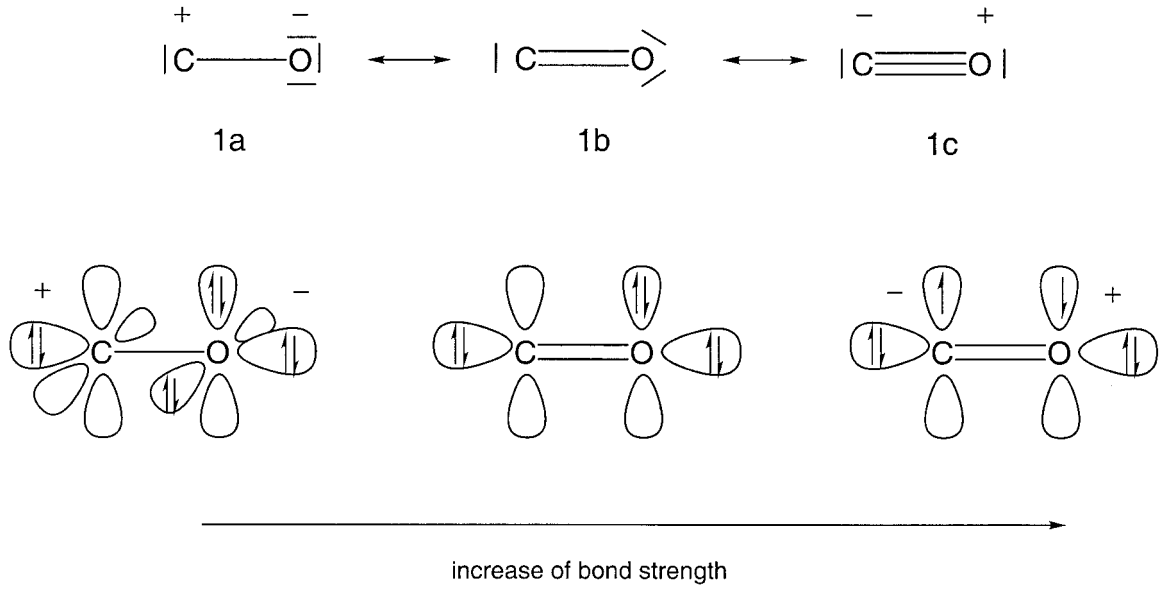

Scheme 1.

Both WFT and KS-DFT use the energy of a single-determinant wavefunction as reference. This reference function is optimized with respect to the total energy for HF, while in KS theory the reference function is optimized to provide the best $\rho(\mathbf{r})$, which means that the reference energy is more positive for KS than for HF; hence the exact KS correlation energy is larger (by its absolute value) than the exact correlation energy in WFT. This agrees with the fact that the approximate correlation functionals in practical DFT calculations generally lead to higher correlation energies (in absolute value) than one gets from WFT calculations for the same system (see below). On the other hand, as the density is the key quantity in DFT and the KS reference system has to reproduce the electron density of the real system, one should expect that the impact of the DFT correlation functional on the density is lower than that of electron correlations in WFT. Altogether, an investigation of the question posed in the title of this work implies that not just the correlation effects of DFT methods are compared with the results of standard WFT methods, but also that the difference between HF and DFT exchange is analysed to point out which correlation effects are already simulated by the particular choice of an X functional.

In previous work, we analysed correlation effects with the help of the electron density distribution $\rho(\mathbf{r})$ calculated for a given molecule at a given level of theory and then compared it with the $\rho(\mathbf{r})$ obtained at another level of theory (using the same geometry, basis set, etc.) thus leading to the analysis of the difference electron density distributions $\Delta\rho(\mathbf{r}) = \rho(\text{method I}) - \rho(\text{method II})$ [30, 31]. In this work, we follow the same approach because a density based theory is best analysed via its $\rho(\mathbf{r})$ distribution, which provides a global impression and is more informative than single values of selected molecular properties such as energy, geometry, etc.

Also, we do not select a large group of molecules to be investigated, but constrain the analysis to a single molecule, the properties of which are highly sensitive to the electron correlation effects covered by a given WFT or DFT method. Such a molecule is carbon monoxide, $CO(^1\Sigma^+)$ (**1**), in its ground state. As shown in scheme 1, the electronic structure of **1** can be described by three resonance structures, **1a**, **1b**, and **1c**, where a dominance of **1b** and **1c** determines the true electronic structure of **1**. If, however, a given method artificially overestimates **1a** or **1c**, a long or short CO bond will be predicted. Hence, **1** represents a sensitive antenna for the electron correlation effects covered by a given method and, therefore, it can be used to identify correlation effects covered by DFT.

2. Computational details and strategy of analysis

Standard HF, MP [5, 6] and CC theory [7, 8, 16, 17] with unfrozen core and analytical energy gradients [31] was employed throughout this work. The response density distribution and other response properties were calculated together with the geometry as was described previously. [30] Electron density and difference electron density distributions were calculated at the experimental geometry of **1** [32] while dissociation energy D_e, dipole moment μ, and atomic charges q were determined at the calculated equilibrium bond length r_e and then compared with the corresponding experimental values

Table 2. Composition of the hybrid functionals used in this work according to

$$E_{XC} = A_{HF}E_X^{HF} + A\left(E_X^{LDA} + B\Delta E_X^{GGA}\right) + E_C^{LDA} + C\Delta E_C^{GGA}$$
$$= A_{HF}E_X^{HF} + D_X^{loc}E_X^{LDA} + D_X^{non-loc}\left(E_X^{LDA} + \Delta E_X^{GGA}\right) + D_c^{loc}E_C^{LDA} + D_C^{non-loc}\left(E_C^{LDA} + \Delta E_C^{GGA}\right)$$

The following sum rules should hold to correctly reproduce the limit of the HEG:

$$A_{HF} + A = 1$$
$$A_{HF} + D_X^{loc} + D_X^{non-loc} = 1$$
$$D_C^{loc} + D_C^{non-loc} = 1.$$

	Exchange		Correlation						Exchange			Correlation		
									HF	DFT		DFT		
Functional	Local	Non-local	Local	Non-local	A_{HF}	A	B	C		Local	Non-loc	Local	Non-loc	Ref.
B3P86	S	B	VWN	P86	0.200	0.800	0.900	0.810	20	8	72	19	81	[26]
B3PW91	S	B	PW91	PW91	0.200	0.800	0.900	0.810	20	8	72	19	81	[26]
B3LYP	S	B	VWN	(LYP − VWN)	0.200	0.800	0.900	0.810	20	8	72	19	81	[26]
B1LYP	S	B	LYP	LYP	0.250	0.750	1.000	1.000	25	0	75	0	100	[27, 28]
mPW1PW91	S	mPW	PW91	PW91	0.250	0.750	1.000	1.000	25	0	75	0	100	[21]
BH&H	S	—	LYP	LYP	0.500	0.500	0.000	1.000	50	50	0	0	100	[29]

[32–34]. The natural bond orbital (NBO) analysis was used to evaluate atomic charges [35].

The DFT functionals employed reach from local density approximation (LDA) to general gradient approximation (GGA) and hybrid functionals; they are listed and described in tables 1 and 2 [18–29]. As for the hybrid functionals, we use a representation somewhat different from that in literature since we want to clarify the amount of HF exchange, local DFT (DFT-local), and non-local DFT (DFT-nonloc) exchange in the X functional and the amount of local and non-local correlation in the C functional (see table 2).

All calculations were carried out with Pople's 6-311+G(3df) basis set, [36], which is of VTZ quality, contains three sets of five d-type polarization functions, one set of seven f-type polarization functions, and is augmented by a set of diffuse sp functions. Calculations were done with the quantum chemical program packages Cologne99 [37], Gaussians98 [38], and Aces II [39].

The analysis of electron correlation effects was performed in five steps. First, typical effects involving two-, three- or more-electron correlation effects were described with a set of difference electron density distributions $\Delta\rho(\mathbf{r}) = \rho(\text{method I}) - \rho(\text{method II})$. In a second step, exchange-only DFT calculations were carried out and the corresponding $\rho(\mathbf{r})$ compared with the electron density distributions determined in the first step. Then, the influence of the C functional was analysed by using $\Delta\rho(\mathbf{r}) = \rho(\text{DFT} - \text{XC}) - \rho(\text{DFT} - \text{X})$ differences and relating the density patterns observed to features calculated with WFT methods (step III). In step IV, we analysed the electron density generated by hybrid functionals focusing on the question how the composition of the functional improves the description of electron interactions. Finally, summing up the effects found for all functionals, a comparison of DFT with correlation corrected WFT methods was given with regard to their ability to correctly describe electron correlation.

3. Correlation effects covered by MP and CC methods

In table 3, energy, equilibrium bond distance, dipole moment, NBO charge at C, and dissociation energy of **1** calculated in this work are listed. A selection of difference electron densities $\Delta\rho(\mathbf{r}) = \rho(\text{method I}) - \rho(\text{method II})$ used for the analysis of electron correlation effects is shown in figure 1. The results of this analysis are given in schematic form in table 4.

The electronic structure of **1** is best described with the help of its molecular dipole moment μ which, contrary to the charge transfer from C to O because of the higher electronegativity χ of O, is directed from the O to the C atom (chemical notation, see scheme 2) thus yielding a negative value [34] (μ values in table 3 and throughout the text are given according to the physical convention). The negative sign of the μ

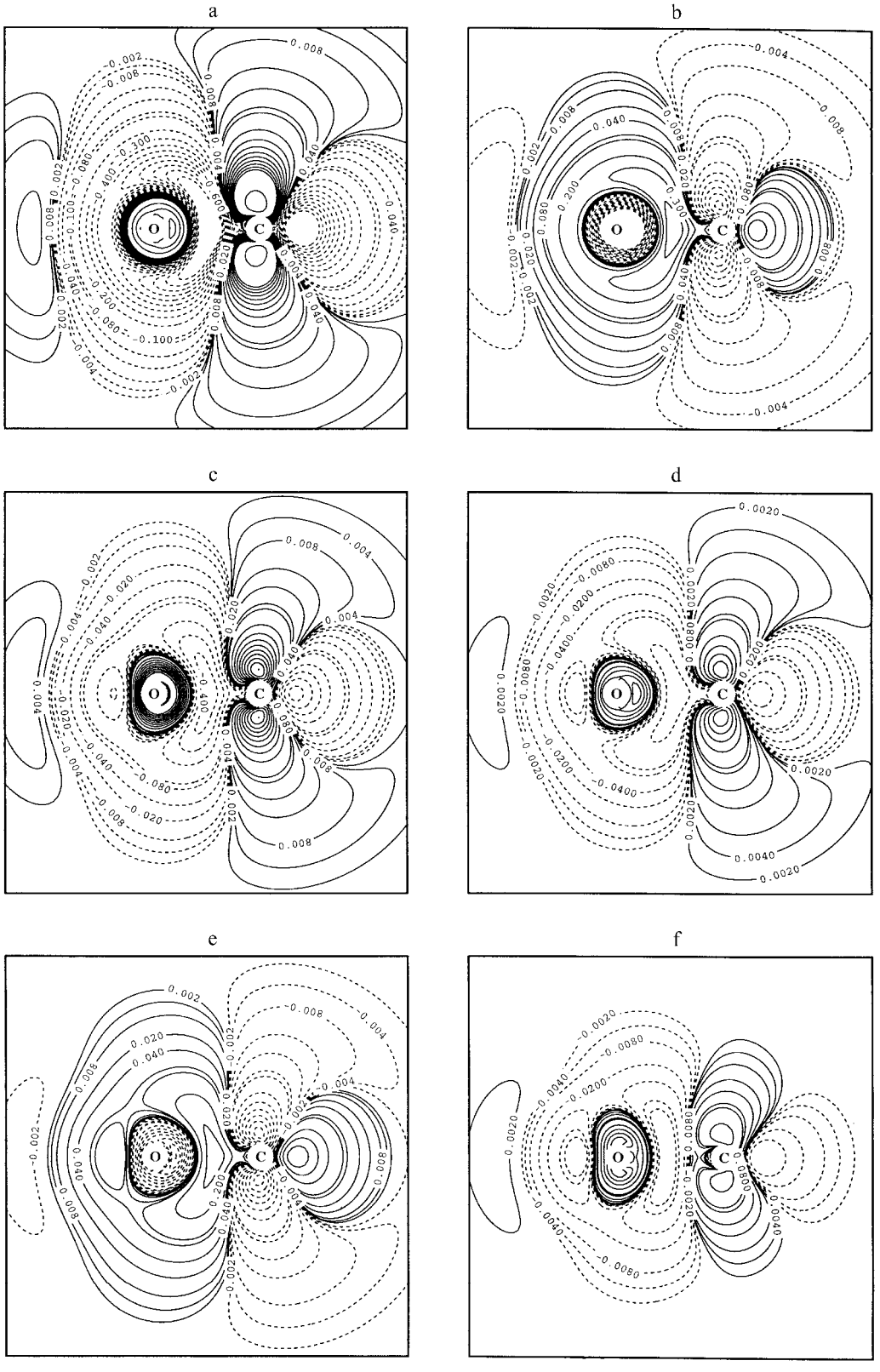

Figure 1. Contour line diagram of the difference electron density distribution $\Delta\rho(\mathbf{r}) = \rho(\text{method I}) - \rho(\text{method II})$ of CO calculated with the 6-311+ G(3df) basis at $r_e(\text{CO}) = 1.128$ Å. Solid (dashed) contour lines are in regions of positive (negative) difference densities. The positions of the C and the O nucleus are indicated. The contour line levels have to be multiplied by the scaling factor 0.01 and are given in $e\,a_0^{-3}$. (*a*) MP2-HF; (*b*) MP3-MP2; (*c*) MP4-MP3; (*d*) MP4(T)-MP4(SDQ); (*e*) CCSD-MP4; (*f*) CCSD-MP3.

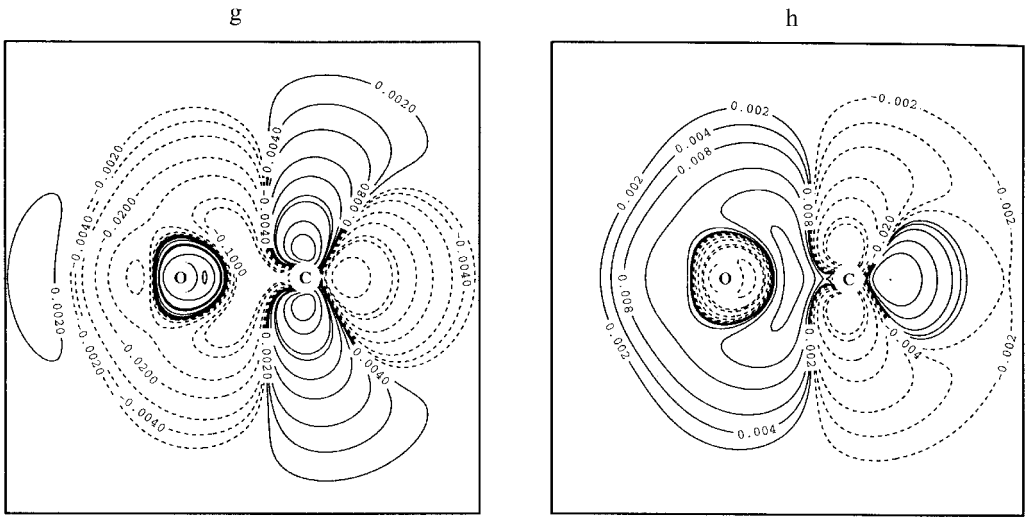

Figure 1. *Continued* (*g*) CCSD(T)-CCSD; (*h*) [CCSD(T)-CCSD]-[MP4-MP4(SDQ)].

Table 3. Total energies E, dissociation energy D_e, equilibrium bond length r_e, dipole moment μ, and atomic charge q of CO calculated at different levels of theory.[a]

Method	Energy			D_e	r_e	μ	q(C)
	CO	C (^{3}P)	O (^{3}P)				
HF	−112.782 78	−37.690 73	−74.810 96	176.4	1.102	0.147	0.583
MP2	−113.207 93	−37.785 15	−74.993 81	269.2	1.133	−0.265	0.432
MP3	−113.205 19	−37.800 84	−75.008 71	248.3	1.117	−0.086	0.481
MP4(SDQ)	−113.213 99	−37.804 23	−75.009 82	251.0	1.127	−0.115	0.468
MP4(SDTQ)	−113.236 00	−37.805 62	−75.012 87	262.0	1.140	−0.191	0.453
CCSD	−113.211 41	−37.805 87	−75.010 22	248.1	1.123	−0.080	0.494
CCSD(T)	−113.232 89	−37.808 29	−75.013 86	257.7	1.130	−0.115	0.480
S-only	−111.520 42	−37.110 43	−73.992 21	262.2	1.139	−0.244	0.450
B-only	−112.862 67	−37.687 09	−74.825 71	219.5	1.147	−0.160	0.466
PW91-only	−112.834 98	−37.670 46	−74.805 69	225.0	1.146	−0.159	0.466
mPW91-only	−112.860 92	−37.683 83	−74.823 33	222.0	1.147	−0.158	0.466
SVWN	−112.742 24	−37.579 27	−74.678 19	304.2	1.126	−0.223	0.449
SVWN5	−112.467 61	−37.467 08	−74.523 60	299.3	1.127	−0.226	0.449
BVWN	−114.086 16	−38.157 04	−75.512 86	261.2	1.134	−0.141	0.466
BVWN5	−113.811 41	−38.044 76	−75.358 19	256.3	1.135	−0.143	0.466
BPL	−113.805 13	−38.040 19	−75.351 22	256.9	1.136	−0.143	0.466
BP86	−113.356 60	−37.845 78	−75.083 43	268.2	1.136	−0.182	0.460
BPW91	−113.346 74	−37.845 40	−75.080 64	264.0	1.135	−0.189	0.457
BLYP	−113.347 12	−37.846 03	−75.082 93	262.4	1.136	−0.156	0.464
B3P86	−113.595 65	−37.953 15	−75.224 98	262.0	1.123	−0.116	0.484
B3PW91	−113.307 07	−37.836 57	−75.061 96	256.4	1.124	−0.124	0.482
B3LYP	−113.359 63	−37.858 52	−75.093 23	256.0	1.124	−0.096	0.487
mPW1PW91	−113.320 74	−37.842 45	−75.073 36	254.1	1.122	−0.109	0.487
BH&H	−112.628 56	−37.556 80	−74.655 04	261.5	1.108	−0.047	0.513
Expt				259.3	1.128	−0.112	

[a] Absolute energies in E_h, dissociation energy in kcal mol^{-1}, bond lengths in Å, dipole moments in D and charge transfer in e. Experimental values from [32–34].

Table 4. Analysis of difference electron density distributions (Compare with figure 1).[a]

	Method	Reference	Correlation effects newly introduced	Consequences: Special	Consequences: General	Properties
1		HF	only exchange correlation	$q(C) \rightarrow q(O)$	MOs contracted $\Delta\chi$ larger	$\mu > 0$; $\lvert\mu\rvert$ large, q large r_e short, D_e small
2	MP2	HF	(a) left–right pair correlation (b) angular pair correlation (c) in–out pair correlation	$\pi(O) \rightarrow \pi(O)$ $\sigma(O) \rightarrow \pi(C)$ $n(X) \rightarrow \text{in} + \text{out}$	MOs expand $\Delta\chi$ smaller	$\mu < 0$, $\lvert\mu\rvert$ large q smaller r_e longer, D_e larger
3	MP3	MP2	reduction of pair correlation	$\pi(O) \leftarrow \pi(C)$ $\sigma(O) \leftarrow \pi(C)$ $n(X) \leftarrow \text{in} + \text{out}$	MOs shrink $\Delta\chi$ larger	$\lvert\mu\rvert$ too small, correct sign q large r_e smaller D_e too small
4	MP4(SDQ)	MP3	orbital relaxation disconnected 4e-correlation	$\pi(O) \rightarrow \pi(C)$ $\sigma(O) \rightarrow \pi(C)$ $n(X) \rightarrow \text{in} + \text{out}$	MOs expand $\Delta\chi$ smaller	$\lvert\mu\rvert$ correct q smaller r_e almost correct D_e still too small
5	MP4	MP4(SDQ)	three-electron correlation	$\pi(O) \rightarrow \pi(C)$ $\sigma(O) \rightarrow \pi(C)$ $n(X) \rightarrow \text{in} + \text{out}$	MOs expand $\Delta\chi$ smaller	$\lvert\mu\rvert$ too large q smaller r_e larger D_e still too small
6	MP4	MP3	sum of 4 and 5			
7	CCSD	MP3	pair correlation corrected by infinite order effects infinite order S effects	$\pi(O) \rightarrow \pi(C)$ $\sigma(O) \rightarrow \pi(C)$ $n(X) \rightarrow \text{in} + \text{out}$	small effects	$\lvert\mu\rvert$, q, D_e comparable with MP3 or larger
8	CCSD	MP4(SDQ)	see 7	$\pi(O) \leftarrow \pi(C)$ $\sigma(O) \leftarrow \pi(C)$ $n(X) \leftarrow \text{in} + \text{out}$	MOs shrink $\Delta\chi$ larger	q larger $\lvert\mu\rvert$, r_e, D_e smaller
9	CCSD(T)	CCSD	(infinite order three-electron correlation effects)	$\pi(O) \rightarrow \pi(O)$ $\sigma(O) \rightarrow \pi(C)$ $n(X) \leftarrow \text{in} + \text{out}$	MOs expand $\Delta\chi$ smaller	$\lvert\mu\rvert$, r_e, D_e larger and almost correct q smaller
10	T(CCSD)	T(MP4)	see 9	$\pi(O) \leftarrow \pi(C)$ $\sigma(O) \leftarrow \pi(C)$ $n(X) \leftarrow \text{in} + \text{out}$	MOs shrink $\Delta\chi$ larger	see 9

[a] For explanation of abbreviations, see text.

value of **1** can be explained by realizing that the molecular dipole moment comprises the effects of both the charge transfer moment (depending on $\Delta\chi$) and the atomic dipole moments (depending on the polarization of the density of the atom in the molecule), as is nicely described by the virial partitioning method of Bader [40]. Because of the electronegativity difference $\Delta\chi(O—C) = \chi(O)—\chi(C)$, the density in the CO bond region is shifted toward the O nucleus, the lone pair density at C becomes more contracted, and that at O more diffuse, as is indicated in scheme 2. The atomic dipole moments, which one can calculate, e.g. with the virial partitioning method, are oriented opposite to the charge transfer moment, thus compensating for it and reducing the magnitude of the molecule dipole moment μ [40, 41]. Calculation of the terms adding to μ at a correlation corrected *ab initio* level reveals that the atomic dipole moments determine the direction of μ leading to the experimental value of -0.112 debye [34] and an orientation opposite to that of the charge transfer moment.

The correct description of μ(CO) requires electron correlation [42–44], where the calculated dipole moment together with the atomic charges sensitively reflects the influence of the correlation effects added at a given level of theory. The failure of HF [30, 42] is due to its exaggerating the effective electronegativity difference between O and C, thus predicting too large a charge transfer from C to O. The dipole moment is oriented in the wrong direction, the bond length becomes too short (strong shielding of the O nucleus, reduction of nuclear repulsion), and admixture of the

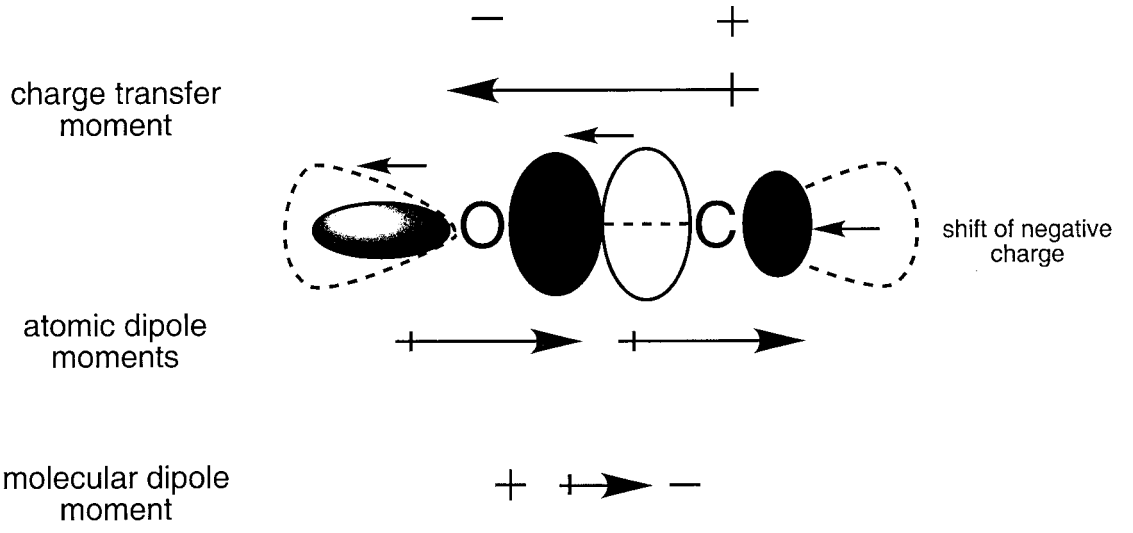

Scheme 2.

ionic term **1a** in scheme 1 leads to a weakening of the bond (table 4).

Changes caused by MP2. MP2 introduces electron pair correlation effects (left–right, angular, in–out), which lead to an expansion of the MOs and a reduction of the effective $\Delta\chi$ between C and O (table 4). Relative to the HF electron density distribution three major changes can be observed (figure 1(*a*)). (a) Left–right correlation causes charge transfer particularly in the π space from the O to the C atom. (b) Angular correlation supports the first effect by shifting negative charge from the region of the σ bond close to the O to the π region at C. (c) In–out correlation shifts part of the charge in the outer valence region closer to the nucleus (inner valence region) in particular at O while another part is moved into the van der Waals region, by which the σ electron lone pairs at C and O become more diffuse.

The net effect is that C receives back some of the negative charge lost at the HF level of theory thus reducing its positive charge, strongly reducing the charge transfer moment and reverting the sign of the molecular dipole moment, which, however, is again exaggerated with regard to its magnitude. Left–right correlation dominates correlation corrections at the MP2 level and, therefore, a characteristic lengthening of the CO bond length is calculated at this level of theory (table 3). Admixture of the ionic structure **1a** is suppressed and **1b** and even **1c** (scheme 1) get increased weight. Because of contributions of **1c**, the calculated dissociation energy D_e becomes too large relative to the experimental value. As is well known, MP2 exaggerates pair correlation effects, thus overcorrecting all molecular properties and leading to opposite extremes relative to HF results.

Changes caused by MP3. MP3 introduces a coupling between D excitations and, accordingly, reduces the degree of pair correlation considerably. In this way, changes in the electron density distribution as well as in the molecular properties are corrected back into the direction of the corresponding HF values (see figure 1(*b*) and 3 in table 4).

Changes caused by MP4. The changes in $\rho(\mathbf{r})$ found at the MP4 level (figure 1(*c*), $4+5=6$ in table 4) are parallel to those found at the MP2 level (figure 1(*a*)). Inspection of the effects introduced by the T excitations reveals that the MP4–MP3 difference density distribution is dominated by three-electron correlation effects, which similar as pair correlation effects lead to a back-transfer of negative charge to the C atom. Actually, the corrections caused by S, D, and Q excitations at MP4 and analysed by $\Delta\rho(\mathrm{MP4(SDQ)}) = \rho(\mathrm{MP4(SDQ)}) - \rho(\mathrm{MP3})$ (see 4 in table 4) are also similar to those observed at MP2 but less strong, so that corrections due to S, D, and Q excitations at the MP4 level are between those obtained at the MP2 and the MP3 level.

Changes caused by CCSD. The correlation effects covered at the CCSD level include infinite order orbital relaxation and pair correlation effects, which means that an exaggeration of pair correlation is avoided. The changes caused by using the CCSD approach can be assessed by comparing either with MP3 or MP4(SDQ), which all contain a corrected pair correla-

tion description (see 7, 8 in table 4). The difference density plots show that CCSD transfers more negative charge back to the C atom than MP3 but less than MP4(SDQ), which indicates that pair correlation effects are still exaggerated at the MP4(SDQ) level. Furthermore, the data of table 3 indicate that the CCSD description of **1** is closer to that of MP3 than that of MP4(SDQ), which is in line with observations made for large scale calculations of molecular geometries and other properties [45]. Compared with MP4, CCSD increases the charge in the π and lone-pair regions at O since the T effects of MP4 are not covered and higher T effects are covered only in the form of disconnected T contributions [14, 15].

Changes caused by CCSD(T). Basically, CCSD(T) leads to the same changes relative to CCSD as MP4 does relative to MP4(SDQ) (compare figures 1(*d*) and (*g*), see also 9 in table 4). However, there are also some important differences with regard to the T effects at CCSD(T) and MP4. The three-electron correlation effects described by T excitations provide an important mechanism to avoid electron clustering at the O atom and to transfer negative charge back to the C atom. These effects can be described as combinations of left–right, angular, and in–out correlations involving three electrons. If the T effects are introduced independently of each other as done at the MP4 level, then some new electron clustering, although less than in the case of pair correlation at the MP2 level, is generated, which can only be avoided by TT coupling effects [14, 15]. CCSD(T) covers about 77% of the infinite order effects in the T space, in particular DT and TT coupling effects, which help to avoid an exaggeration of three-electron correlation as it occurs at the MP4 level [14, 15]. This is confirmed by the difference density $\rho(\mathrm{T}(\mathrm{CCSD}(\mathrm{T}))) - \rho(\mathrm{T}(\mathrm{MP4}))$ (see figure 1(*h*)), which shows that the T effects at MP4 exaggerate the charge transfer back to the C atom and other effects accompanied by this. CCSD(T) provides the most accurate description of the properties of **1**, as is confirmed by the calculated molecular properties listed in table 3.

In summary, figure 1(*a–h*) and table 4 reveal that the stepwise addition of higher correlation effects in MP or CC theory leads to an oscillation of molecular properties and typical features of the electron density distribution, which has also been observed for many other molecules and molecular properties [6, 13, 30, 31]. Apart from this, figure 1 and table 4 provide a list of typical electron correlation effects, which are used in the following to analyse electron correlation as covered by various density functionals.

4. What is covered by DFT exchange functionals?

In figure 2, the electron density distribution determined in exchange-only DFT calculations is compared with that of HF, MP, and CC calculations where Becke exchange [19] was used as the appropriate standard applied today in nearly all routine DFT calculations. The difference electron density distribution $\Delta\rho(B\text{-}\mathrm{HF}) = \rho(\mathrm{B\text{-}only}) - \rho(\mathrm{HF})$ (figure 2*a*) reveals changes in the charge distribution of **1** which qualitatively agree with those obtained for $\Delta\rho(\mathrm{MP2}) = \rho(\mathrm{MP2}) - \rho(\mathrm{HF})$ (figure 1(*a*)), i.e. charge is transferred from the π space at O and the $\sigma(\mathrm{CO})$ region to the $\pi(\mathrm{C})$ space; also negative charge is shifted from the σ lone pair regions either towards the nuclei or out into the van der Waals region.

A direct comparison with $\rho(\mathbf{r})$ of MP2 (figure 2(*b*)) confirms that the B exchange functional leads to a similar electron density distribution as MP2, although the negative charge is more contracted to the nuclei and out into the van der Waals region thus depleting the valence region (indicated by the dashed lines). Actually, the $\rho(\mathbf{r})$ of the B-only calculation is also close to the density distributions obtained at MP4 and CCSD(T) (figure 2(*d*, *f*)) while clearly it differs from those calculated at HF, MP3, and CCSD (figure 2(*a*, *c*, *e*)). Analysis of the profile plots shown in figure 3 actually reveals that in bond and lone pair regions the B-only density is closest to the MP4 density distribution, which is also confirmed by the calculated r_e (1.147 Å), μ (−0.16 D), and q (0.453, table 3). Deviations from MP2 or CCSD(T) are larger than MP4 deviations where one has to consider that small differences integrated over the total bond and valence region can lead to considerable differences in calculated properties.

The B-only dissociation energy (219.5 kcal mol^{-1}) is larger than the HF value (176.4 kcal mol^{-1}, table 3) but 30–50 kcal mol^{-1} smaller than the values from correlation-corrected WFT methods and 40 kcal mol^{-1} smaller than the experimental value (259.3 kcal mol^{-1}, [33]). By contrast, the S-only dissociation energy is 262.5 kcal mol^{-1} and differs only by 3 kcal mol^{-1} from the experimental value. This is in line with the observation that the exchange hole in LDA resembles the XC hole and that this resemblance is closer for LDA than for GGA functionals, which of course does not mean that X-only LDA is a method with high overall accuracy: on the contrary, the S-only value for the dipole moment (−0.244 D versus −0.112 D experimentally, table 3) indicates that the LDA description is insufficient.

The strong increase of the B-only density in the nuclear region is an artefact characteristic for gradient-corrected exchange and correlation functionals. The cusp of the electron density at a nucleus leads to a

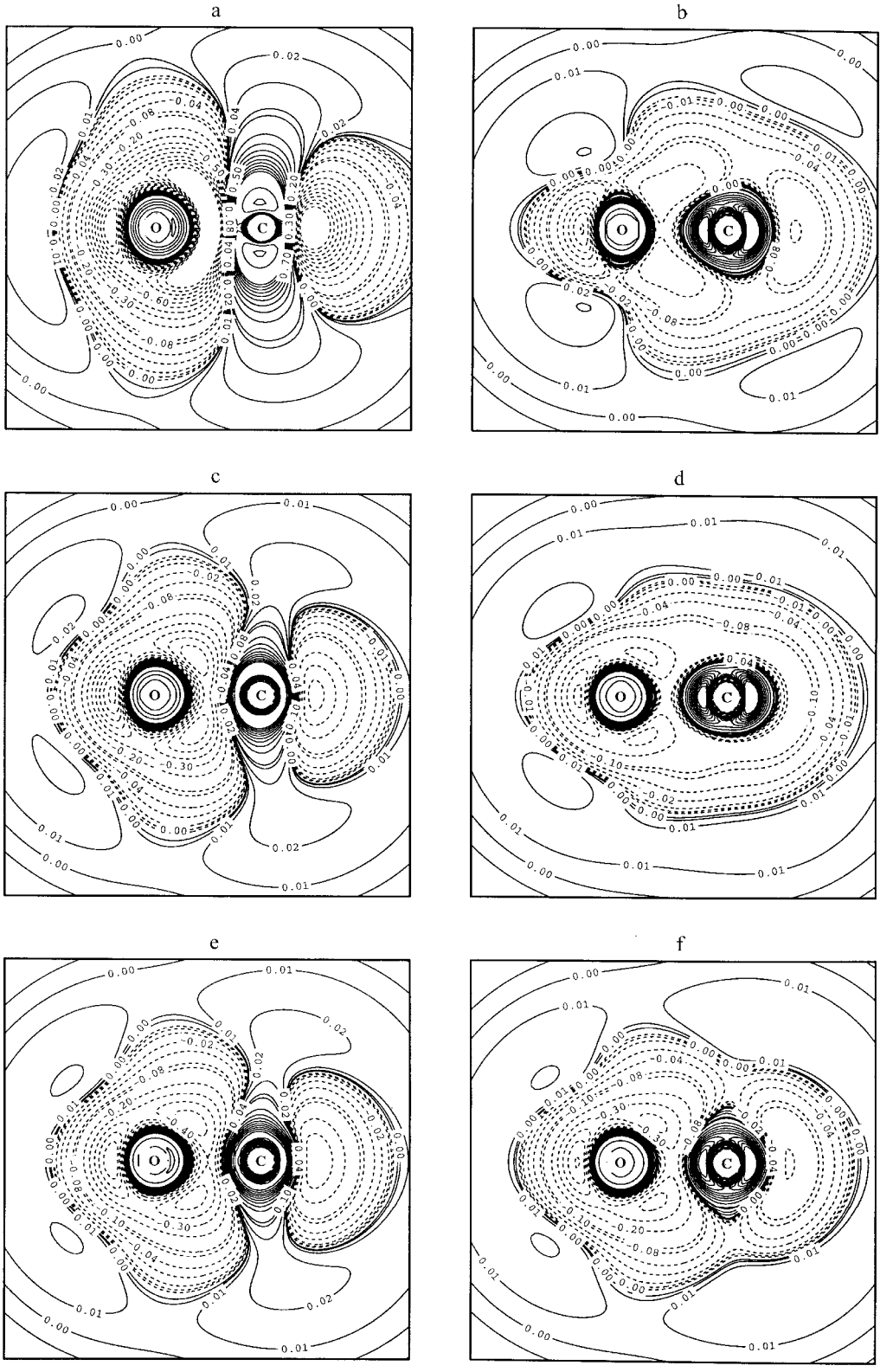

Figure 2. Contour line diagram of the difference electron density distribution $\Delta\rho(\mathbf{r}) = \rho(\text{method I}) - \rho(\text{method II})$ of CO calculated with the 6-311+G(3df) basis at $r_e(\text{CO}) = 1.128$ Å. Solid (dashed) contour lines are in regions of positive (negative) difference densities. The positions of the C and the O nucleus are indicated. The contour line levels have to be multiplied by the scaling factor 0.01 and are given $e\,a_0^{-3}$. (*a*) B-only-HF; (*b*) B-only-MP2; (*c*) B-only-MP3; (*d*) B-only-MP4; (*e*) B-only-CCSD; (*f*) B-only-CCSD(T).

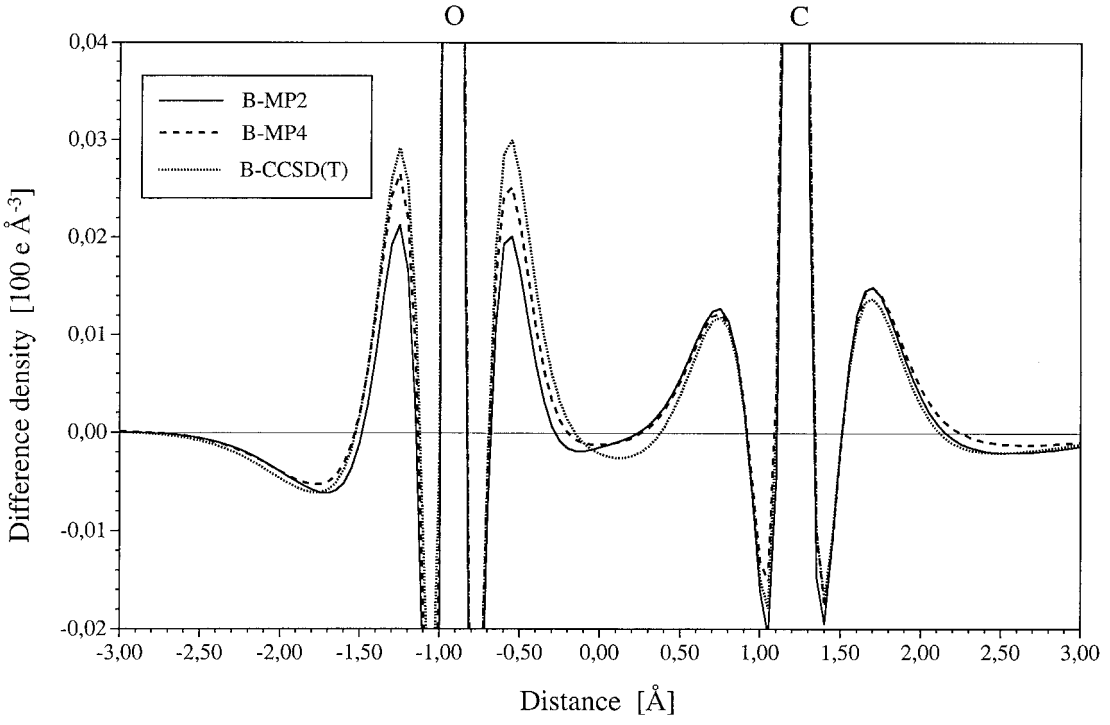

Figure 3. Profile plot of the difference electron density distribution $\Delta\rho(\mathbf{r}) = \rho(\text{method I}) - \rho(\text{method II})$ of CO calculated with the 6-311+G(3df) basis at $r_e(\text{CO}) = 1.128$ Å and taken along the CO axis. The positions of the C and the O nucleus are indicated. (*a*) B-only-MP2; (*b*) B-only-MP4; (*c*) B-only-CCSD(T).

singularity in the gradient of the density, which in turn results in a singularity in the exchange or correlation potential. The gradient corrections to the exchange functionals increase the absolute value of the exchange energy, and the corresponding contribution to the exchange potential is therefore attractive [46]. The density cusps at the nuclei thus lead to an attractive singular contribution to the exchange potential, which increases the effective nuclear charge and the electronegativity. The strongest influence of this extra potential is to be seen for the core orbitals, which are contracted compared with LDA, leading to an increase in charge density immediately at the nucleus and a decrease in the surrounding region. This generates a shell structure in the X-only density distribution (compare with figure 3), the origin of which is mathematical rather than physical.

Other exchange functionals investigated in this work (see table 1) lead to similar difference density plots to those shown in figures 2 and 3. Therefore, the various exchange functionals were compared directly to determine differences in the description of DFT exchange (figure 4).

Figure 4(*a*) shows that Slater exchange [18] increases the density in the bond region, in the van der Waals region, and also in the inner valence regions of the two atoms. These observations are in line with the fact that LDA functionals overestimate the bond density and by this the bond strength ($r_e = 1.139$ Å compared with 1.147 Å, table 3). The PW91 exchange functional is comparable with the B exchange functional in its effect on $\rho(\mathbf{r})$ (figure 4(*b*)) except that it shifts more negative charge into the inner valence and into the van der Waals region. The mPW91 exchange functional takes some of the density from the inner to the outer valence region; however, changes are very small.

In table 5, which complements figure 4, the effects of different exchange functionals are further characterized by directly comparing them, i.e. using the first X-only density distribution as a reference and determining those molecular regions in which the density is increased by the second X-only functional. For this purpose, the molecular region is schematically dissected into core, inner valence, outer valence, bond, and van der Waals region where the bond region, of course, is largely identical to parts of the outer valence regions located between the atoms. In table 6, calculated X energies are listed, which reveal that HF exchange is absolutely seen larger than S exchange, but slightly smaller than GGA exchange (B, PW91, mPW91) in the case of **1**, where this observation is generally valid.

In summary, the inclusion of correlation effects at MP2, MP4 or even CCSD(T) qualitatively leads to the same density changes as the replacement of HF exchange by DFT exchange, no matter whether this is

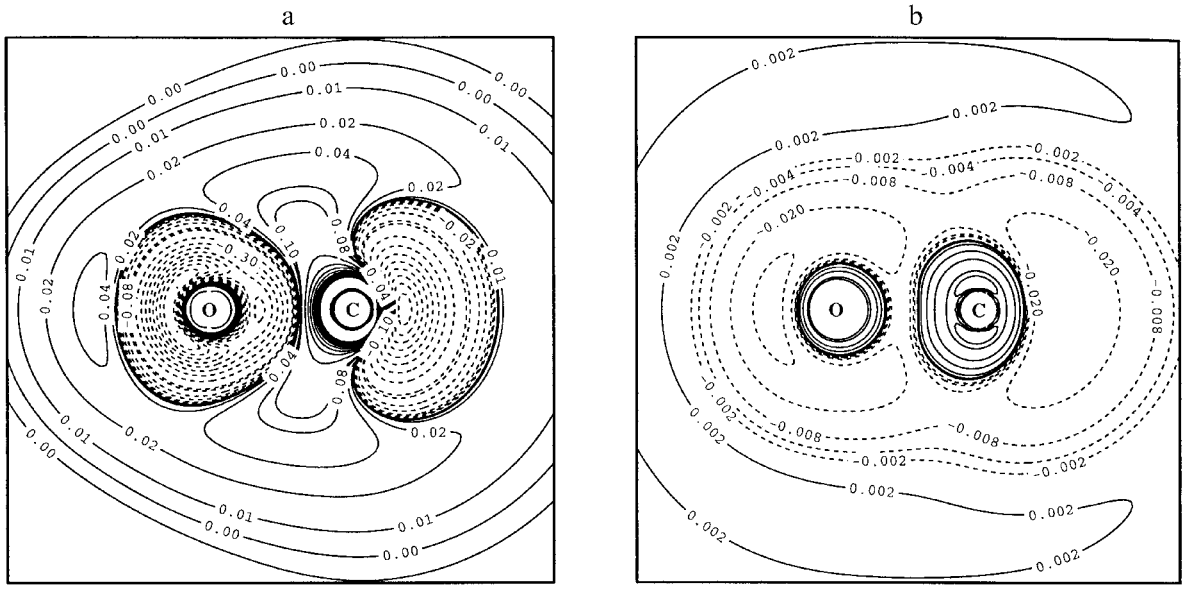

Figure 4. Contour line diagram of the difference electron density distribution $\Delta\rho(\mathbf{r}) = \rho(\text{method I}) - \rho(\text{method II})$ of CO calculated with the 6-311+G(3df) basis at $r_e(\text{CO}) = 1.128$ Å. Solid (dashed) contour lines are in regions of positive (negative) difference densities. The positions of the C and the O nucleus are indicated. The contour line levels have to be mutliplied by the scaling factor 0.01 and are given in $e\,a_0^{-3}$. (*a*) S–B exchange; (*b*) PW91–B exchange.

Table 5. Analysis of electron density distributions as obtained with different exchange and correlation functionals.[a]

	Method	Reference	Changes in electron density: Core	Inner	Outer	Bond	vdW	Changes in properties
	Exchange functionals							
E1	S	B	s	l	s	l	l	stronger bond, shorter r_e repulsive vdW interactions
E2	S	PW91	s		similar to E1			similar to E1
E3	S	mPW91	s		similar to E1			similar to E1
E4	PW91	B	s	l	s	s	l	more shielding of nuclei somewhat stronger bond
E5	mPW91	PW91	l	(s)	(l)	(s)	—	very small differences, shift to outer valence sphere decrease of bond strength
	Correlation functionals							
S1	BLYP	B	s	l	l	l	s	strong increase in bond strength; less vdW repulsion
S2	BVWN5	B	l		similar to S1			similar to S1
S3	BPL	B	l		similar to S1			similar to S1
S4	BP86	B	l	s	l	l	s	very strong bond
S5	BPW91	B	s		similar to S4			similar to S4
S6	BLYP	BVWN5	0	s/l	s/l	s	l	weaker bonding more vdW repulsion
S7	BP86	BPL	s	s	s	s	l	S7–S9: reduction of density
S8	BP86	BVWN5	s	s	s	s	0	in core and valence region
S9	BPW91	BVWN5	ss	s	s		0	
S10	BVWN5	BVWN	s	s	s	s	l	very small differences

[a] The following notation is used: s (smaller), (s) (very small s), ss (much smaller), l (larger), (l) (very small l), 0 (negligible difference), s/l (smaller at O, larger at C); vdW (van der Waals).

Table 6. Exchange and correlation energies of CO obtained with different functionals at the experimental geometry.[a]

Exchange		Correlation		Correlation	
Method	Energy	Method	Energy	Method	Energy
HF	−13.328 96	VWN	−1.225 34	MP2	−0.426 79
S	−11.963 03	VWN5	−0.950 33	MP3	−0.423 79
B	−13.381 70	PL	−0.943 97	MP4(SDQ)	−0.432 91
PW91	−13.349 78	P86	−0.495 25	MP4(SDTQ)	−0.454 61
mPW	−13.378 39	PW91	−0.485 72	CCSD	−0.430 28
		LYP	−0.485 32	ΔT	−0.018 42
				CCSD(T)	−0.448 70
B3LYP	−13.269 98	B3LYP	−0.625 66		
B3PW91	−13.272 14	B3PW91	−0.573 63		
B3P86	−13.273 09	B3P86	−0.862 15		
mPW1PW91	−13.375 72				
BH&H	−12.645 81				
Total electron interaction energy					
MP2	−13.755 75	MP4(SDQ)	−13.761 86	CCSD	−13.759 23
MP3	−13.752 75	MP4(SDTQ)	−13.783 56	CCSD(T)	−13.777 65
SVWN	−13.225 14	BLYP	−13.883 59	B3PW91	−13.845 77
SVWN5	−12.946 84	PW91PW91	−13.854 20	B3P86	−14.135 24
BP86	−13.891 94	mPWPW91	−13.883 20	mPW1PW91	−13.862 18
BPW91	−13.886 92	B3LYP	−13.895 64	BH&H	−13.130 56

[a] All energies are given in E_h. Exchange energies were obtained with X-only calculations; correlation energies with the B exchange functional.

done at the LDA or GGA level. It would be misleading to interpret these similarities in the way that DFT exchange already covers Coulomb electron correlation effects as one might assume because the exchange energy is absolutely seen larger for GGA functionals than for HF. However, HF and DFT theory set two different reference points with regard to exchange and, therefore, HF and KS exchange are not directly comparable. On the other hand, it seems to be a fact that, even though the DFT exchange functional does not include any Coulomb correlation effects by construction, it simulates orbital relaxation, pair correlation, and even three-electron correlation effects with respect to the electron density in calculations for finite systems.

The LDA description of the exchange hole assumes a model exchange hole that is spherically symmetric at every point of the molecule, independent of the actual chemical environment of this point. This unspecified form of the model exchange hole mimics dynamic pair correlation effects in the molecule, as Becke discussed for the H_2 molecule [26] and, therefore, it is qualitatively more similar to the exact exchange and correlation hole than to the HF exchange hole. Adding gradient corrections to the Slater exchange functional corrects the form of the model exchange hole slightly towards the form of the exact exchange hole but does not lead to qualitative changes. Thus, DFT exchange favours density enhancement and depletion in different regions of the molecule in a similar way to that in which exchange and pair correlation together do in WFT, which explains the similarities between X-only DFT densities on the one hand and the MP2, MP4 or CCSD(T) density on the other hand. However, the profile plots of figure 3 along the bond axis show clearly that beyond this qualitative similarities in the bond and valence region X-only and WFT descriptions differ strongly in the nuclear regions, reflecting the different starting points of DFT and WFT methods.

5. The effects covered by correlation functionals

The addition of pair, three-, and higher-order-electron correlation effects at the MPn level leads in general to an extension of the orbitals, to a more diffuse charge distribution, and to typical changes in molecular properties, as for example a lengthening of the bond [6]. The introduction of coupling between electron correlation effects always reduces these trends. This is the reason why (because of the presence of infinite order effects) a perfectly coupled many-body method such as CCSD leads to less extended orbitals, a less diffuse charge distribution, and to somewhat shorter bond lengths than either MP2 or MP4(SDQ). In general, one can say that the inclusion of higher-order correlation effects (where higher order implies both increase in the number of

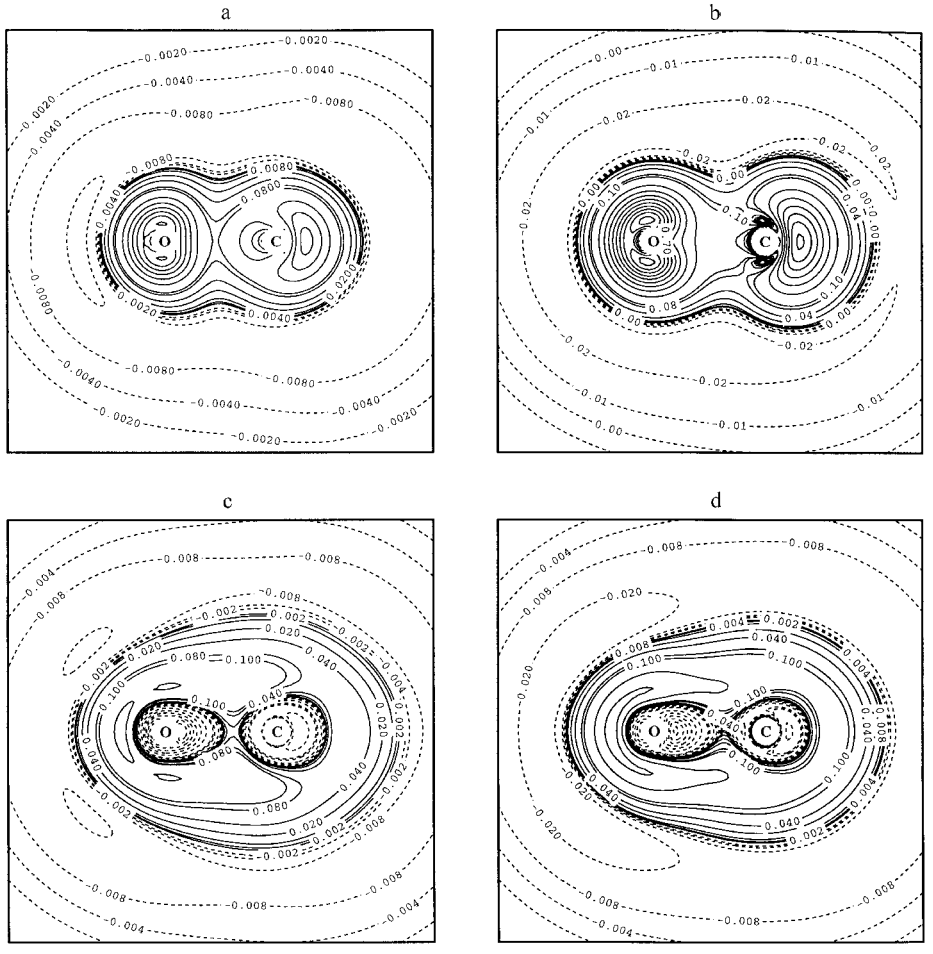

Figure 5. Contour line diagram of the electron density distribution $\rho(\mathbf{r})$ of CO calculated for various correlation functionals with the 6-311+G(3df) basis at $r_e(\mathrm{CO}) = 1.128$ Å. Solid (dashed) contour lines are in regions of positive (negative) difference densities. The positions of the C and the O nucleus are indicated. The contour line levels have to be multiplied by the scaling factor 0.01 and are given in $e\,a_0^{-3}$. (*a*) LYP functional; (*b*) VWN5 functional; (*c*) P86 functional; (*d*) PW91 functional.

correlating electrons and increase in the number of coupling effects) often reduce those effects obtained with lower order correlation effects.

At the LDA level, electron correlation is described by an attractive local potential that becomes stronger the higher the density is. The incorporation of an LDA correlation functional will therefore transfer electronic charge from regions with low electron density into regions with high electron density, i.e. the charge density will be enhanced in the core and bonding regions and depleted in the outer valence and van der Waals regions. As the correlation potential depends on the local density only, this charge transfer will be less specific than the charge transfer due to the explicit inclusion of electron correlation in WFT.

Contrary to the case of exchange correlation, the neglect of density variations in LDA leads to an exaggeration of correlation effects. The inclusion of gradient corrections corrects this exaggeration and makes the correlation potential less attractive, in particular in regions with a high density gradient. At the nuclei, the GGA contribution to the correlation potential becomes singular for the same reasons as the GGA contribution to the exchange potential. The singularity for the correlation potential is repulsive and partly compensates for the attractive singularity of the exchange potential. The main impact of the gradient corrections on the correlation potential is thus that charge is transferred back from the core and bond regions into the outer valence regions of the molecule, which slightly reduces the effects of the LDA correlation potential.

The influence of the correlation potential on the charge distribution is thus similar to the influence higher-order correlation effects have in WFT. For example, charge is transferred from the outer valence and in particular van der Waals region into the core and

valence region. This can be seen, e.g. for the LYP functional (figure 5(*a*)), which leads to a contraction of the density thus increasing $\rho(\mathbf{r})$ in the valence and core region, but decreasing it in the outer valence and in particular in the van der Waals region. Consequently, the bond length of **1** is shortened from 1.147 Å (HF) to 1.136 Å (BLYP, table 3) and the bond strength is increased, actually overshooting the experimental D_e value slightly (262.4 kcal mol^{-1} versus 259.3 kcal mol^{-1}, table 3).

It is interesting to note that the VWN5 correlation functional of LDA theory leads to a $\Delta\rho(\text{VWN5}) = \rho(\text{BVWN5}) - \rho(\text{B-only})$ (figure 5(*b*)) distribution that resembles the corresponding LYP distribution (figure 5(*a*)) the only significant difference being a somewhat larger amount of density shifted into the bond region which leads to a slightly shorter bond length (1.135 Å, table 3). We used the VWN5 functional as reference considering that this is based on the more accurate QMC investigation of the HEG (table 1) and covers all higher-order correlation effects of the latter. However, differences in $\rho(\text{VWN5})$ with regard to $\rho(\text{VWN})$ are tiny, in particular in the core region, because the two functionals, even though derived with different methods, have similar properties for high densities. VWN5 moves some minor amount of density from the bonding and valence region out into the van der Waals region which, according to the observations made in WFT, reflects the fact that higher-order correlation effects are covered by the QMC derivation of VWN5 [22]. Also, the PL functional shows hardly any difference with regard to the VWN5 functional because these two functionals are just different parametrizations of the QMC data (see table 1).

The P86 [23, 24] and PW91 [20] correlation functionals are constructed in a way differing from both that of the VWN, [22] PL [23] or LYP functional [25] and, accordingly, the $\Delta\rho(\mathbf{r})$ pattern of the former functionals somewhat deviates from those of the latter functionals (figure 5(*c*, *d*)) although density is again shifted from the van der Waals region into the valence region and in a limited way also to the bonding region. There are, however, large depletion areas surrounding the atoms in the inner valence region where the effects of these changes are counteracting the increase in density caused by the X functional (figure 3) and avoiding too much electron clustering in these regions. Basically, BLYP [19, 25], BP86 [19, 23, 24], and BPW91 [19, 20] results are similar for **1**, which suggests that the major effect is caused by the contraction of the more diffuse electron density distribution obtained at the exchange-only DFT level (as for additional comparisons of correlation functionals, see table 5).

Clearly, the correlation functionals correct deficiencies of the X functionals, where corrections are of course much smaller than the actual changes caused by the latter. This simply reflects the fact that exchange correlation is much larger than Coulomb correlation (the X energy represents 96.5% of the total XC correlation energy in the case of BLYP; compare with table 6) and that the X hole is just somewhat corrected by the much smaller correlation hole. Nevertheless, these corrections have important effects which remind us of the higher-order dynamic electron correlation effects of WFT. For example, the C functional removes density out of the van der Waals region, thus decreasing exchange (overlap) repulsion between closed-shell molecules and giving dispersion effects a better change to stabilize a potential van der Waals complex. Comparison with the MP2, MP4 or CCSD(T) densities both for B-only (figure 3) and BLYP calculations shows that this removal of charge is still not sufficient, and probably this is responsible for the fact that GGA functionals perform poorly when applied to van der Waals complexes [47].

The correlation energies listed in table 6 reveal that GGA reduces their absolute magnitude by 50% so that they become comparable with WFT correlation energies. Nevertheless, the LYP Coulomb correlation energy is still 8% larger for **1** than the CCSD(T) correlation energy, while the total electron interaction energies for BLYP and CCSD(T) differ by 89 mE_h, the DFT value being 0.6% larger.

Relative to LDA, GGA corrected functionals such as BLYP [19, 25] perform reasonably, although they do not reach CCSD(T) quality [4]. In section 6 we analyse how hybrid functionals can further improve DFT data.

6. Changes in correlation caused by hybrid functionals

In general, correlation effects decrease electronegativity differences $\Delta\chi$ between unlike atoms and, by this, the polarity of bonds formed by these atoms. One can explain this by considering the fact that Coulomb electron correlation always leads to an expansion of the molecular orbitals and to a more diffuse charge distribution, i.e. negative charge is not contracted so strongly towards the nuclei, indicative of a lower effective electronegativity. In WFT, an underestimation of the effective $\Delta\chi$ parallel to a strong suppression of the ionic terms of HF theory can lead to serious problems when describing molecules composed of strongly electronegative atoms, as was recently demonstrated for FOOF [48].

Similar problems occur at the DFT level, where the X functional already mimics typical Coulomb electron correlation effects. Clearly, there is a need to reintroduce ionic effects and to increase the effective $\Delta\chi$. In the case of **1**, this means that some charge has to be back-

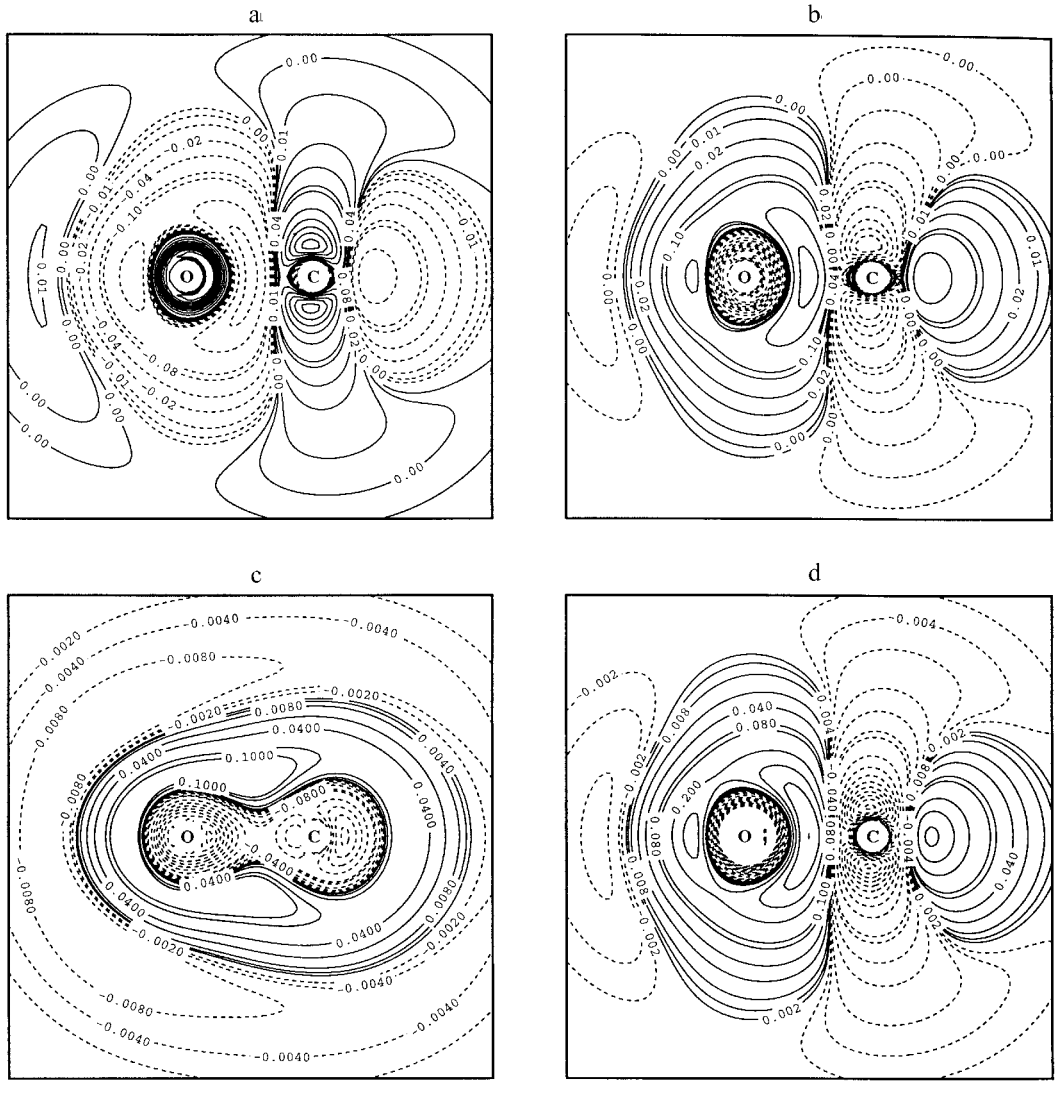

Figure 6. Contour line diagram of the difference electron density distribution $\Delta\rho(\mathbf{r}) = \rho(\text{method I}) - \rho(\text{method II})$ of CO calculated with the 6-311+G(3df) basis at $r_e(\text{CO}) = 1.128$ Å. Solid (dashed) contour lines are in regions of positive (negative) difference densities. The positions of the C and the O nucleus are indicated. The contour line levels have to be multiplied by the scaling factor 0.01 and are given in $e a_0^{-3}$. (*a*) B3LYP – BLYP; (*b*) B3PW91 – BPW91; (*c*) B3LYP – B3PW91; (*d*) BH+HLYP – B3LYP.

transferred from the C to the O atom to reduce the dominating effect of the atomic dipole moments, to pack more density around the O nucleus, to shorten the bond by this, and to correct the exaggeration of the dissociation energy typical of LDA descriptions but still disturbing for GGA functionals.

In figure 6 various hybrid functionals are compared with their corresponding GGA counterparts, where in the following we focus first on B3LYP [26]. As expected, the major effect of mixing in 20% HF exchange is the redistribution of charge from the $\pi(\text{C})$ to the $\pi(\text{O})$ space due to the increased $\Delta\chi$ difference. But there is also a depletion of charge in the van der Waals region and a building up of more density in the bonding and the outer valence rather than the inner valence region of the atoms. Clearly, the latter effects have to do with the admixture of 8% local exchange and 19% local correlation (see table 2).

The consequences for **1** and its properties are obvious (B3LYP: $r_e = 1.124$ Å, $\mu = -0.096$ D, $D_e = 256.0$ kcal mol^{-1}, table 3) where calculated data reached almost CCSD(T) quality. The various hybrid functionals all generate similar changes in $\rho(\mathbf{r})$ and the other properties of **1** (see figure 6(*a*, *b*)), where the charge transfer to the

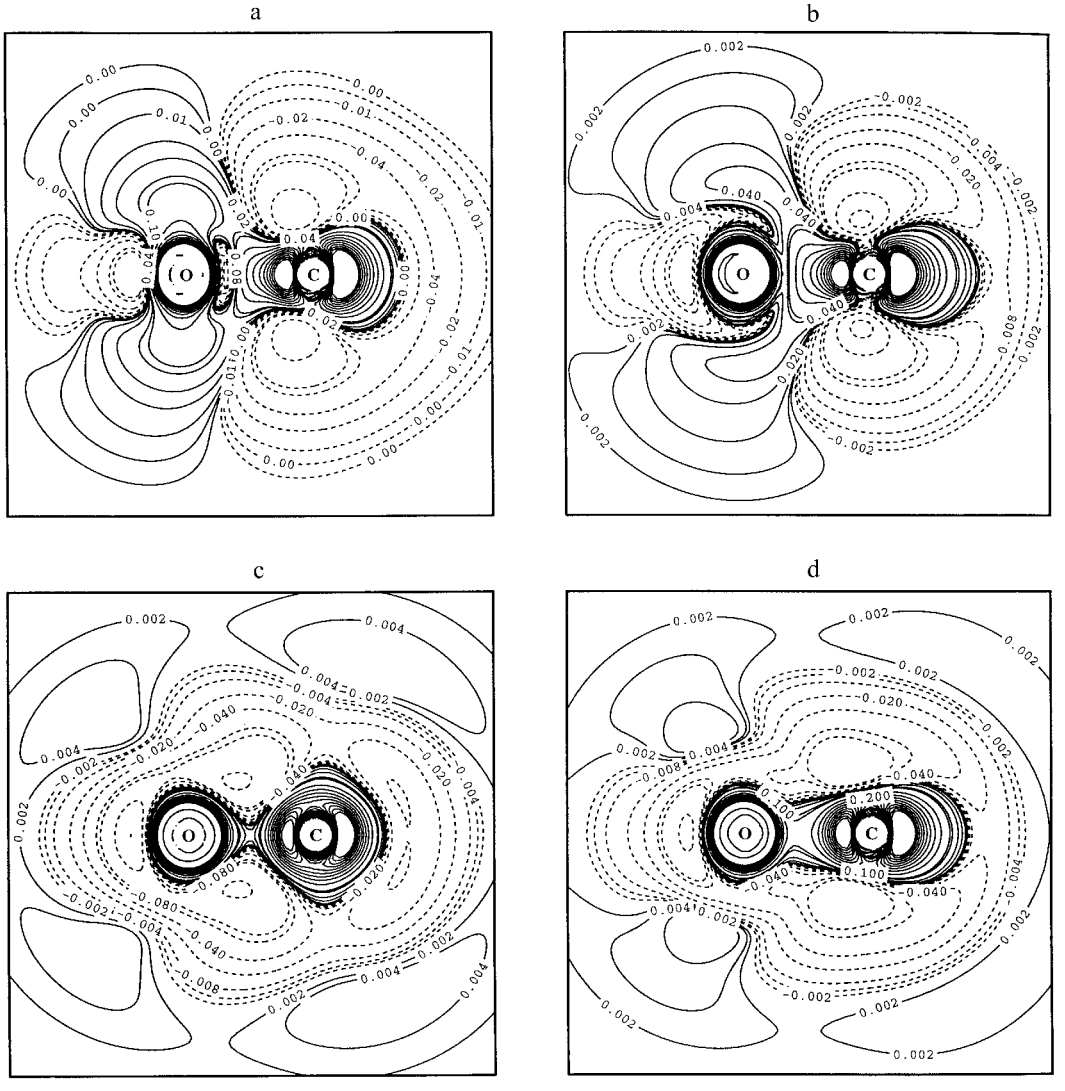

Figure 7. Contour line diagram of the difference electron density distribution $\Delta\rho(\mathbf{r}) = \rho(\text{method I}) - \rho(\text{method II})$ of CO calculated with the 6-311+G(3df) basis at $r_e(\text{CO}) = 1.128$ Å. Solid (dashed contour lines are in regions of positive (negative) difference densities. The positions of the C and the O nucleus are indicated. The contour line levels have to be mutliplied by the scaling factor 0.01 and are given in $e\,a_0^{-3}$. (*a*) B3LYP – MP2; (*b*) B3LYP – MP4; (*c*) B3LYP – CCSD; (*d*) B3LYP – CCSD(T).

O atom of course becomes stronger the more HF exchange is mixed in (BH&H, figure 6(*d*)) [29]. B3LYP increases relative to B3PW91 the density in the bond region and the inner valence region, which should lead to a stronger bond but which is not reflected in the calculated properties of **1** (table 3).

It is interesting to compare $\rho(\mathbf{r})$ obtained with B3LYP directly with the WFT reference densities as in figure 7. Although B exchange leads to a density close to the corresponding MP4 density, this is no longer true for the B3LYP density because of the admixture of HF exchange and local X/C functionals (figure 7(*b*)). There is also a considerable difference between the B3LYP and MP2 densities (figure 7(*a*)) while there is now a closer similarity to CCSD and even the CCSD(T) density distribution of **1** (figure 7(*c*, *d*)). This is also reflected by the calculated properties of **1** (table 3), where the B3LYP values are bracketed by the CCSD and CCSD(T) values. The D_e(B3LYP) value (256.0 kcal mol^{-1}, table 3) is closer to the CCSD(T) rather than the CCSD value; however, for bond length, atomic charges, and dipole moment the situation is reversed. Clearly, the hybrid functionals provide the best description of **1**, reaching almost the quality of the CCSD(T) description.

7. Conclusion

A number of conclusions can be drawn from the present investigation.

(1) All X functionals investigated in this work already contain effects that are actually reminiscent of pair and three-electron correlation effects introduced by MP2 and MP4 in WFT. Indeed, the best agreement between B-only and WFT calculations is found at MP4, while MP2 and CCSD(T) show similarities also.

(2) The major difference between the B-only and a WFT density is found in the core and inner valence region where B-only largely exagerates the value of the electron density. This can be traced back to a singularity of GGA functionals at the nucleus, which leads to a strong attraction of electron density towards the nucleus and an artificial shell structure in the density close to the nucleus. This is the major reason why GGA-exchange leads to poor molecular properties for **1**.

(3) Local exchange leads to a higher density in the bond region relative to the density obtained with B exchange. Therefore, the bond strength is exaggerated by local exchange.

(4) All correlation functionals contract the density towards the bond and valence region, thus taking negative charge out of the van der Waals region and improving the description of van der Waals interactions. This is typical of the coupling effects contained in higher order MPn and CC methods, i.e. correlation functionals contain by their construction correlation effects not (or only partially) present in MP2, MP3 or MP4.

(5) Correlation functionals also reduce an accumulation of density in the inner valence region and correct in this way the typical deficiency of the GGA exchange functionals.

(6) Similar to correlation corrected WFT methods, BLYP and other GGA functionals underestimate ionic terms needed for a correct description of polar bonds. This is compensated for in hybrid functionals by mixing in 20 to 25% HF exchange. The balanced mixing (achieved by fitting DFT results to empirical data) of local and non-local X and C effects leads to a strengthening of polar bonds, so that B3LYP gives the best account of all DFT methods with regard to the molecular properties of **1**.

(7) DFT with the BLYP or B3LYP functional covers pair correlation effects beyond those present at MP2 or MP4. A comparison of B3LYP with WFT methods reveals that the density of B3LYP is similar to that of CCSD and CCSD(T). The special composition of the hybrid functional B3LYP guarantees that both higher-order pair–pair coupling effects (contained in CCSD) and a fairly large portion of three-electron correlation effects (contained in CCSD(T)) are mimicked. In this way calculated molecular properties are more accurate than CCSD results, and reach in some cases the accuracy of CCSD(T) calculations [4].

(8) In view of the results obtained in this work it seems no longer justified to compare DFT methods such as B3LYP with MP2, as often is done in the literature. Clearly, DFT results cover correlation effects only covered by CC methods, and by this they should be compared with CCSD and CCSD(T).

(9) In view of the fact that the calculation of the properties of **1** and their sensitive dependence on a proper account of electron correlation requires a high accuracy method, results obtained in this work provide a basis for assessing the accuracy of DFT calculations for a given chemical problem.

This work was supported by the Swedish Natural Science Research Council (NFR). Calculations were performed on the supercomputers of the Nationellt Superdatorcentrum (NSC), Linköping, Sweden. The authors thank the NSC for a generous allotment of computer time.

References

[1] HOHENBERG, P., and KOHN, W., 1994, *Phys. Rev.* B, **136,** 864.

[2] KOHN, W., and SHAM, L., 1965, *Phys. Rev.* A, **140,** 1133.

[3] For reviews on DFT methods, see, e.g. PARR, R. G. and YANG, W., 1989, *Density-Functional Theory of Atoms and Molecules* (Oxford University Press); LABANOSWSKI, J. K., and ANDZELM, J. W., 1990, *Density Functional Methods in Chemistry* (Heidelberg: Springer-Verlag); SEMINARIO, J. M., and POLITZER, P. 1995, *Modern Density Functional Theory—A Tool For Chemistry* (Amsterdam: Elsevier); CHONG, D. P., 1997, *Recent Advances in Density Functional Methods*, Part II (Singapore: World Scientific); DOBSON, D. F., VIGNALE, G. and DAS, M. P., 1998, *Electronic Density Functional Theory, Recent Progress and New Directions* (New York: Plenum Press); LÖWDIN, P.-O., 1980, *Density Functional Theory* (New York: Academic Press).

[4] See, e.g. B. B. LAIRD, R. B. ROSS and T. ZIEGLER, 1996, *Chemical Applications of Density Functional Theory* (Washington, DC: American Chemical Society); JOUBERT, D., 1997, *Density Functionals: Theory and Applications* (Heidelberg: Springer-Verlag); GILL, P., 1998, *Encyclopedia of Computational Chemistry*, Vol. 1, edited by SCHLEYER, P. V. R., ALLINGER, N. L., CLARK, T., GASTEIGER, J., KOLLMAN, P. A., SCHAEFER III, H. F., SCHREINER, P. R. (Chichester, UK: Wiley); and references therein. See also KRAKA, E., SOSA, C. P., and CREMER, D., 1996, *Chem. Phys. Lett.*, **260,** 43; GUTBROD, R., KRAKA, E., SCHINDLER, R. N. and CREMER, D., 1997, *J. Amer. chem. Soc.*, **119,** 7330; GRÄFENSTEIN, J., KRAKA, E. and CREMER, D., 1998, *Chem. Phys. Lett.*, **288,** 593; D. Cremer, E. Kraka, and P. G. Szalay, 1998, *Chem. Phys. Lett.*, **292,** 97; GRÄFENSTEIN, J., HJERPE, A., KRAKA, E. and CREMER,

D., 2000, *J. phys. Chem.* A, **104,** 1748; KRAKA, E. and CREMER, D., 2000, *J. Amer. chem. Soc.*, in press.
[5] MØLLER, C., and PLESSET, M. S., 1934, *Phys. Rev.*, **46,** 618.
[6] For a recent review see CREMER, D., 1998, *Encyclopedia of Computational Chemistry*, Vol. 3, edited by SCHLEYER, P. v. R., ALLINGER, N. L., CLARK, T., GASTEIGER, J., KOLLMAN, P. A., SCHAEFER III, H. F. and SCHREINER, P. R. (Chichester: Wiley) p. 1706.
[7] For a recent review see GAUSS, J., 1998, *Encyclopedia of Computational Chemistry*, Vol. 1, edited by SCHLEYER, P. v. R., ALLINGER, N. L., CLARK, T., GASTEIGER, T., KOLLMAN, P. A., SCHAEFER III, H. F. and SCHREINER, P. R. (Chichester: Wiley) p. 615.
[8] BARTLETT, R. J., and STANTON, J. F., 1994, *Reviews in Computational Chemistry*, Vol. 5, edited by LIPKOWITZ K. B. and BOYD, D. B. (Weinheim: VCH) p. 65; CREMER, D. and Zhi He, 1997, *Conceptual Perspectives in Quantum Chemistry*, Vol. III, edited by CALAIS, J.-L. and KRYUACHKO, E. (Dordrecht: Kluwer) p. 239.
[9] WERNER, H.-J., 1987, *Ab Initio Methods in Quantum Chemistry*, Vol. II, edited by LAWLEY, K. P. (New York: Wiley) p. 1; SZALAY, P. G. and BARTLETT, R. J. 1983, *Chem. Phys. Lett.*, **214,** 481; SZALAY, P. G., 1997, *Modern Ideas in Coupled-Cluster Methods*, edited by BARTLETT, R. J. (Singapore: World Scientific) p. 81.
[10] HE, Z., and CREMER, D., 1996, *Intl. J. Quantum Chem.*, **59,** 15, 31, 57, 71.
[11] CREMER, D., and HE, Z., 1996, *J. phys. Chem.*, **100,** 6173; D. Cremer, and Z. He, 1997, *J. molec. Struct. Theochem*, **398–399**, 7.
[12] HE, Y., and CREMER, D., 2000, *Molec. Phys.*, in press.
[13] FORSBERG, B., HE, Z., HE, Y., and CREMER, D., 2000, *Intl. J. Quantum Chem.*, **76,** 306.
[14] HE, Z., and CREMER, D., 1991, *Intl. J. Quantum Chem. Symp.*, **25,** 43.
[15] HE, Z., and CREMER, D., 1993, *Theoret. Chim. Acta*, **85,** 305.
[16] PURVIS III, G. D., and BARTLETT, R. J., 1982, *J. chem. Phys.*, **76,** 1910.
[17] RAGHAVACHARI, K., TRUCKS, G. W., POPLE, J. A., and HEAD-GORDON, M., 1989, *Chem. Phys. Lett.*, **157,** 479.
[18] SLATER, J., 1951, *Phys. Rev.*, **81,** 385.
[19] BECKE, A. D., 1988, *Phys. Rev.* A, **38,** 3098.
[20] PERDEW, J. P., 1991, *Electronic Structure of Solids '91*, edited by ZIESCHE, P. and ESCHRIG, H. (Berlin: Akademie-Verlag) p. 11; PERDEW, J. P. and WANG, Y., 1992, *Phys. Rev.* B, **45,** 13 244; PERDEW, J. P. and WANG, Y., 1992, *Phys. Rev.* B, **45,** 13 244.
[21] ADAMO, C., and BARONE, V., 1998, *J. chem. Phys.*, **108,** 664.
[22] VOSKO, S. H., WILK, L., and NUSAIR, M., 1980, *Can. J. Phys.*, **58,** 1200.
[23] PERDEW, J. P., and ZUNGER, A., 1981, *Phys. Rev.* B, **23,** 5048.
[24] PERDEW, J. P., 1986, *Phys. Rev.* B, **33,** 8822.
[25] LEE, C., YANG, W., and PARR, R. G., 1988, *Phys. Rev.* B, **37,** 785.
[26] BECKE, A. D., 1993, *J. chem. Phys.*, **98,** 5648.
[27] BECKE, A. D., 1996, *J. chem. Phys.*, **104,** 1040.
[28] ADAMO, C., and BARONE, V., 1997, *Chem. Phys. Lett.*, **272,** 242.
[29] BECKE, A. D., 1993, *J. chem. Phys.*, **98,** 1372.
[30] KRAKA, E., GAUSS, J., and CREMER, D., 1991, *J. molec. Struct. Theochem*, **234,** 95.
[31] GAUSS, J., and CREMER, D., 1992, *Adv. Quantum Chem.*, **23,** 205.
[32] HUBER, K. P., and HERZBERG, G. H., 1979, *Molecular Spectra and Molecular Constants of Diatomic Moiecules* (New York: Van Nostrand-Reinhold).
[33] CHASE JR., M. W., DAVIES, C. A., DOWNEY JR., J. R., FRUIP, D. J., MCDONALD, R. A., and SYVERUD, A. N., 1985, *J. Phys. Ref. Data*, **14,** Suppl. 1.
[34] BURRUS, C. A., 1958, *J. chem. Phys.*, **28,** 427.
[35] CARPENTER, J. E., and WEINHOLD, F., 1988, *J. molec. Struct. Theochem*, **169,** 41; REED, A. E. and WEINHOLD, F., 1983, *J. chem. Phys.*, **78,** 4066; REED, A. E., CURTISS, L. A. and Weinhold, F., 1988, *Chem. Rev.*, **88,** 899.
[36] KRISHNAN, R., FRISCH, M., and POPLE, J. A., 1980, *Chem. Phys.*, **72,** 4244.
[37] KRAKA, E., GRÄFENSTEIN, J., GAUSS, J., REICHEL, F., OLSSON, L., KONKOLI, Z., HE, Z., and CREMER, D., 1999, Cologne99, Göteborg University, Göteborg.
[38] FRISCH, M. J., TRUCKS, G. W., SCHLEGEL, H. B., SCUSERIA, G. E., ROBB, M. A., CHEESEMAN, J. R., ZAKRZEWSKI, V. G., MONTGOMERY JR., J. A., STRATMANN, R. E., BURANT, J. C., DAPPRICH, S., MILLAM, J. M., DANIELS, A. D., KUDIN, K. N., STRAIN, M. C., FARKAS, O., TOMASI, J., BARONE, V., COSSI, M., CAMMI, R., MENNUCCI, B., POMELLI, C., ADAMO, C., CLIFFORD, S., OCHTERSKI, J., PETERSSON, G. A., AYALA, P. Y., CUI, Q., MOROKUMA, K., MALICK, D. K., RABUCK, A. D., RAGHAVACHARI, K., FORESMAN, J. B., CIOSLOWSKI, J., ORTIZ, J. V., STEFANOV, B. B., LIU, G., LIASHENKO, A., PISKORZ, P., KOMAROMI, I., GOMPERTS, R., MARTIN, R. L., FOX, D. J., KEITH, T., AL-LAHAM, M. A., PENG, C. Y., NANAYAKKARA, A., GONZALEZ, C., CHALLACOMBE, M., GILL, P. M. W., JOHNSON, B., CHEN, W., WONG, M. W., ANDRES, J. L., GONZALEZ, C., HEAD-GORDON, M., REPLOGLE, E. S., and POPLE, J. A., 1998, Gaussian98, Revision A3 (Pittsburgh PA: Gaussian, Inc.).
[39] STANTON, J. F., GAUSS, J., WATTS, J. D., LAUDERDALE, W. J., and BARTLETT, R. J., 1992, Aces II, Quantum Theory Project, University of Florida; see also STANTON, J. F., GAUSS, J., WATTS, J. D., LAUDERDALE, W. J. and Bartlett, R. J., 1992, *Intl J. Quantum Chem. Symp.*, **26,** 879.
[40] BADER, R. F. W., and NGUYEN-DANG, T. T., 1981, *Rep. Progr. Phys.*, **44,** 893; *Adv. Quantum Chem.*, **14,** 63; BADER, R. F. W., 1981, *The Force Concept in Chemistry*, edited by DEB, B. M. (New York: Van Nostrand Reinhold) p. 39.
[41] KRAKA, E., 1985, Ph.D. thesis, Cologne.
[42] SIU, A. K., and DAVIDSON, E. F., 1970, *Intl J. Quantum Chem.*, **4,** 233; GREEN, S., 1971, *Chem. Phys.*, **54,** 827; F. P. BILLINGSLEY, H. KRAUSS, and M. KRAUSS, 1974, *J. chem. Phys.*, **60,** 4130; KIRBY-DOCKEN, K., and LIU, B., 1977, *J. chem. Phys.*, **66,** 4309; JASIEN, P. G., and DYKSTRA, C. E., 1985, *Intl J. Quantum Chem.*, **28,** 411; JAQUET, R., KUTZELNIGG, W., and STAEMMLER, V., 1980, *Theoret. Chim. Acta*, **54,** 205.
[43] KRISHNAN, R., and POPLE, J. A., 1981, *Intl J. Quantum Chem.*, **20,** 1067; SADLEY, A. J., 1978, *Theoret. Chim. Acta*, **47,** 205.

[44] SCUSERIA, G. E., and SCHAEFER III, H. F., 1988, *Chem. Phys. Lett.*, **148,** 205; WATTS, J., TRUCKS, G. W., and BARTLETT, R. J., 1989, *Chem. Phys. Lett.*, **157,** 359.
[45] CREMER, D., and KRAKA, E., unpublished results.
[46] See, e.g. PERDEW, J. P., BURKE, K., and ERNZERHOF, M., 1996, *Phys. Rev. Lett.*, **77,** 3865; 1997, *Phys. Rev. Lett.*, **78,** 1396.
[47] KRISTYAN, S., and PULAY, P., 1994, *Chem. Phys. Lett.*, **229,** 175; HOBZA, P., SPONER, J., and RESCHEL, T., 1995, *J. comput. Chem.*, **16,** 1315; RUIZ, E., SALAHUB, D. R., and VELA, A., 1995, *J. Amer. chem. Soc.*, **117,** 1141.
[48] KRAKA, E., HE, Y., and CREMER, D., 2000, *J. phys. Chem.*, in press.